

Magnetic Trapping of Cold Methyl Radicals

Yang Liu,¹ Manish Vashishta,¹ Pavle Djuricanin,¹ Sida Zhou,¹ Wei Zhong,² Tony Mittertreiner,¹ David Carty,³ and Takamasa Momose^{1,2}

¹*Department of Chemistry, The University of British Columbia, Vancouver, BC V6T 1Z1, Canada*

²*Department of Physics and Astronomy, The University of British Columbia, Vancouver, BC V6T 1Z1, Canada*

³*Durham University, Joint Quantum Centre Durham - Newcastle,*

Departments of Chemistry and Physics, South Road, Durham DH1 3LE, UK

(Dated: January 13, 2018)

We have demonstrated that a supersonic beam of methyl radicals (CH_3) in the ground rotational state of both *para* and *ortho* species has been slowed down to standstill with a magnetic molecular decelerator, and successfully captured spatially in an anti-Helmholtz magnetic trap for > 1 s. The translational temperature of the trapped CH_3 radicals was about 200 mK. The methyl radical is a non-polar polyatomic molecule, which is predicted to be an ideal system for further cooling below 1 mK *via* sympathetic cooling with ultracold atoms. In addition, it is a highly reactive intermediate that plays an important role in various processes in cold environments such as planetary atmospheres and the interstellar medium. The demonstrated trapping capability of methyl radicals opens up various possibilities for realizing ultracold ensembles of molecules towards Bose-Einstein condensation of polyatomic molecules and investigations of reactions governed by quantum statistics.

PACS numbers: 37.20.+j, 37.10.Mn, 37.10.Pq, 34.50.Cx

Since the realization of Bose-Einstein condensation (BEC) of ultra-cold atoms [1, 2], experimental observation of correlated motion of matter waves of particles in an ensemble has drawn considerable attention in various fields, revealing new quantum aspects of matter. Especially, the research of cold and ultracold molecules has expanded rapidly over the past decade because of their importance in various fields [3–5]. The study of fundamental symmetries in nature such as measuring the electric dipole moment of the electron is one of the benchmark applications of cold molecules in fundamental physics [6, 7]. Reactions of atoms and molecules in the temperature range of 2 K - 100 K are relevant to astronomy [8], yet understanding mechanisms at low temperatures is still challenging. Recent studies on collisions in ultracold KRb [9] and in merged beam experiments [10] have revealed that interactions between molecular matter waves is a completely new regime in collision physics that is governed by quantum statistics [11, 12].

Recent developments in molecular deceleration [13] now make it possible to control the translational motion of molecules and create extremely slow molecular beams. Among various molecules, free radicals having unpaired electron(s) are of interest in relation to cold scattering because of their high reactivity towards other molecules and substances. Since molecules with unpaired electron(s) always have a non-zero magnetic moment, it is natural to use magnetic fields to manipulate the translational motion of these reactive species, i.e. Zeeman deceleration [14–18].

The Zeeman deceleration technique has been initially reported for H and D atoms [14], and metastable Ne [15]. However, due to technical difficulties, O_2 is the only molecule that has been successfully decelerated by

Zeeman deceleration so far [16–18], except for our preliminary work on the deceleration of methyl radicals (CH_3) [19]. Here, we demonstrate that a supersonic beam of CH_3 in the ground rotational state can be fully slowed down by well-controlled pulsed magnetic fields and trapped in a magnetic trap for longer than a second for the first time.

Creating cold ensembles of the methyl radical is of particular interest. It is one of the most important and fundamental intermediates in hydrocarbon chemistry and also plays a key role in reactions at low temperatures in environments such as planetary atmospheres and the interstellar medium [20, 21]. CH_3 does not possess an electric dipole moment [22], and therefore has no radiative excitation levels with photons longer than $7.1 \mu\text{m}$. [23] Molecules with an electric dipole moment such as OH, NH or NH_3 suffer from unavoidable trap loss due to rotational excitations by blackbody radiation [24]. However, there is no such trap loss for CH_3 , making it an ideal system for long trapping experiments which is imperative for the realization of further cooling towards the creation of molecular BEC. It was predicted that the cross section of an inelastic collision between CH_3 and *S*-state atoms is extremely small [25] by virtue of being a symmetric top molecule, which raises the possibility of sympathetic cooling into the ultracold regime (< 1 mK) with ultracold ($< 100 \mu\text{K}$) alkaline-earth metals and perhaps even evaporative cooling. Since CH_3 , having only a permanent magnetic moment, is a different type of molecule from those which have been trapped before, its behavior in the ultracold regime would shed light on anisotropic interactions peculiar to molecules. Another key feature of CH_3 is that it exists as two spin isomers, *para* ($I = 1/2$) and *ortho* ($I = 3/2$), which is an ideal system to

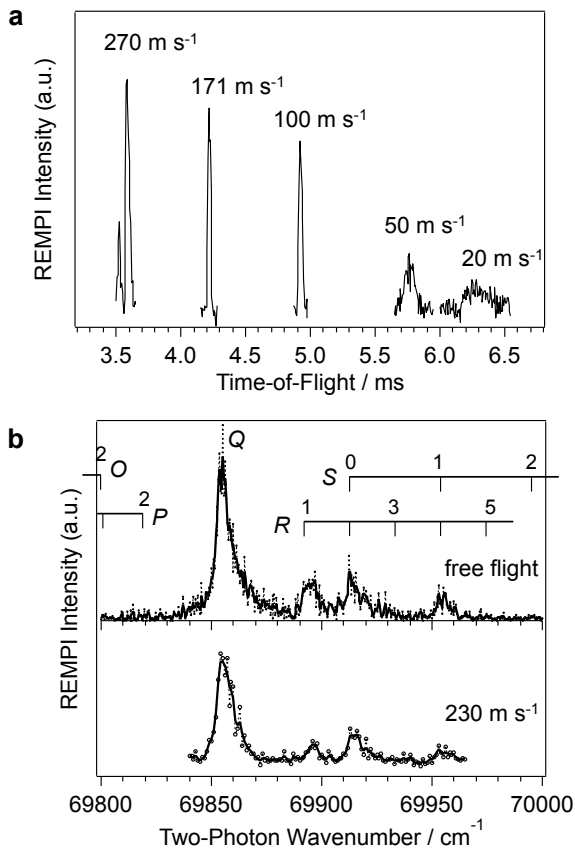


FIG. 1. (a) Time-of-Flight (TOF) feature of decelerated CH_3 beams detected by REMPI. The mean final longitudinal velocities of each decelerated CH_3 packet are shown on top of each peak. A free flight beam of CH_3 (mean velocity 340 m s^{-1}) arrives at the REMPI ionization point at 3 ms after the nozzle opening, which is not shown. (b) A REMPI frequency spectrum of CH_3 in a free flight beam (top) seeded with Kr and in a decelerated beam (bottom, the mean velocity was 230 m s^{-1}). Spectroscopic assignments are given on top of each peak in the top trace with O , P , Q , R , and S corresponding to $\Delta N = -2, -1, 0, 1$ and 2 , respectively.

solve the outstanding problem of understanding the rate and mechanism of nuclear spin conversion between spin isomers [26] as well as the separation of different nuclear spin states of molecules [27–29].

The energy of each rotational state of CH_3 shows an almost identical shift under magnetic fields to those of a free electron due to the decoupling between the electron spin angular momentum, S , and the rotational angular momentum, N , at high magnetic fields ($> 0.5 \text{ T}$) [19]; one shows a monotonical increase in the energy at higher magnetic fields (low-field-seeking (LFS) state), and the other shows a decrease (high-field-seeking (HFS) state). Its shift is approximated by $\Delta E_Z \sim 0.94 B_0 M_S \text{ cm}^{-1}$, where B_0 is the magnitude of the magnetic field (magnetic flux density) in units of tesla and M_S is the pro-

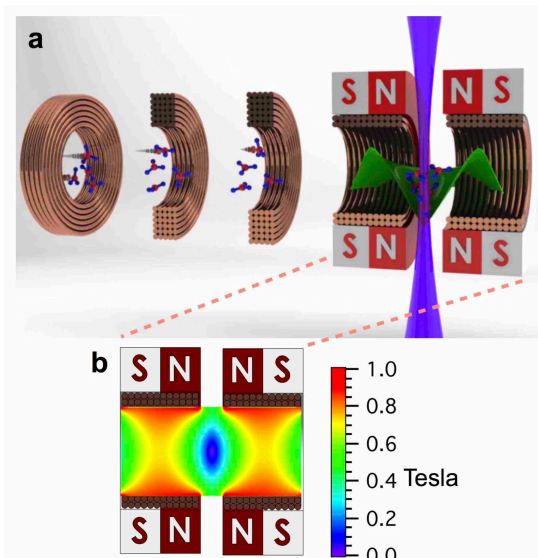


FIG. 2. (a) A schematic drawing of the end of the decelerator showing the last five solenoid coils where the last two are embedded in the trap, which consists of two permanent magnets. A part of the cross section of the trap is shown. The green shape shows the effective potential for the CH_3 radicals in the trap. The purple line shows the laser path for REMPI detection of the trapped radicals. (b) The cross section of the magnetic field distribution inside the trap (in units of Tesla).

jection of the electron spin angular momentum in units of h [19]. Zeeman deceleration uses the LFS state to decelerate the translational motion of molecules by pulsing periodic magnetic fields. In this study, we used a linear magnetic molecular decelerator comprised of 85 solenoid coils for the deceleration of a supersonic beam of CH_3 radicals [18, 19]. Technical details on the stable operation of such a long Zeeman decelerator will be described elsewhere.

A supersonic beam of CH_3 was produced by electric discharge of methane seeded in Kr. By cooling the nozzle down to 150 K , a mean velocity of 340 m s^{-1} was obtained. By adjusting the magnetic field strength produced by the solenoid coils along with the motion of the molecules, a portion of the radicals in the LFS states can be slowed to as low as 20 m s^{-1} , which results in the arrival of the radicals in the detection chamber at a later time than the free flight beam. Examples of the deceleration of molecular beams are shown in Fig. 1(a), where various final mean longitudinal velocities between 270 m s^{-1} and 20 m s^{-1} were obtained.

Resonance enhanced multi-photon ionization spectroscopy (REMPI) frequency spectra [30] showed transitions from $N'' = 0$ ($S(0)$) and $N'' = 1$ ($R(1)$ and $S(1)$) states of CH_3 , but no transitions from rotational states higher than $N'' = 1$ such as $P(2)$, $O(2)$, or $R(3)$ as shown in Fig. 1(b). These spectra indicate that the rotational

cooling of CH_3 radicals during the supersonic expansion was efficient enough to produce only the lowest rotational states of each nuclear spin isomer of *ortho* and *para* selectively. It should be noted that both states are simultaneously decelerated in this experiment, because the Zeeman shift of these two states are almost identical.

In order to trap the decelerated radicals, an anti-Helmholtz type magnetic trap made of two ring-shaped NdFeB permanent magnets was placed at the end of the decelerator. A schematic figure is shown in Fig. 2(a) and its magnetic field distribution is shown in Fig. 2(b). This trap provides a maximum magnetic field of 0.75 T (longitudinal) and 0.45 T (transverse), which corresponds to a 500 mK (longitudinal) and 300 mK (transverse) trap depth for CH_3 . In addition, solenoid coils were placed inside the magnets and worked as the last stages of the decelerator. For trapping experiments, the decelerator was configured such that a target CH_3 radical had a longitudinal velocity of about 60 m s^{-1} before entering the trap region. The last two coils placed inside the magnets were utilized to bring the target CH_3 radical packet to a complete standstill before it reached the middle of the rear magnet. Upon termination of the current flow in the two solenoids, complete trapping of the radical packet between the two permanent magnets was achieved.

Figure 3(a) shows a TOF feature of the REMPI signal of CH_3 at the centre of the trap. A strong REMPI signal was observed at TOF = 7.0 ms – 7.5 ms, which corresponds to the first entry of a dense radical packet into the trap region. After that, signals were detected continuously for $\sim 1 \text{ s}$, which confirms that the decelerated CH_3 radicals were successfully confined in the trap. The observed TOF feature was well reproduced by trajectory simulations of the radicals inside the trap, which is shown as a solid trace in Fig. 3(a).

The trapped signal showed an exponential decay over time. The two traces shown in Fig. 3(b), which were recorded every 100 ms with a 10 Hz pulsed laser, correspond to the cases where the background pressure was 3.8×10^{-9} Torr (filled circle) and 6.3×10^{-9} Torr (filled triangle). The fitted $1/e$ lifetime, τ , of the trapped radicals was $\tau = 1.03 \pm 0.19 \text{ s}$ and $0.70 \pm 0.16 \text{ s}$, respectively.

The shorter trap time at higher background pressure indicates that the trap lifetime of CH_3 is limited by collisions with residual background gases. Under such conditions, the number of trapped radicals, N_{CH_3} , may obey a first order differential equation $dN_{\text{CH}_3}/dt = -(1/\tau)N_{\text{CH}_3}$, where the lifetime, τ , is inversely proportional to the average of the product of the cross section, σ , and velocity, v , of background gas particles [31]. The measurement of background gases by a residual gas analyzer revealed that the major component of the background gas in our vacuum chamber was H_2 with some N_2 as a minor component (less than 1/3 of H_2). By assuming that the trap loss is entirely induced by H_2 molecules ($v=1950 \text{ m s}^{-1}$ mean velocity at 300 K), the

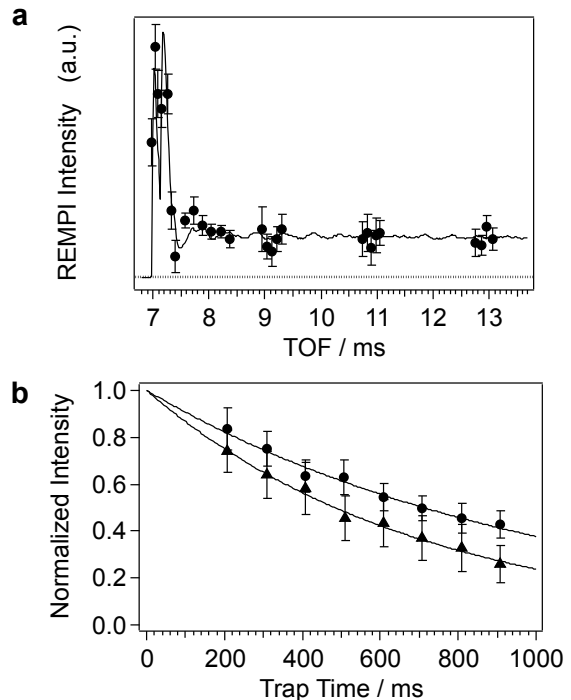


FIG. 3. (a) Observed TOF (filled circle) of trapped CH_3 . The solid trace shows a simulated TOF feature. The baseline is shown as a dotted line. (b) Trapped signal intensity over 1 s normalized to the intensity at TOF = 10 ms for each fitted curve. The background pressure in the trap chamber was 3.8×10^{-9} Torr (filled circle) and 6.3×10^{-9} Torr (filled triangle). The solid lines show fitted curves with a single exponential decay function for each pressure.

average of the cross section for the trap loss caused by H_2 molecules is obtained to be $\langle \sigma \rangle_{\text{H}_2} \sim 380 \text{ \AA}^2$ at the present trap depth of $\sim 400 \text{ mK}$. Further quantitative analyses, however, will require results from on-going experiments in which various foreign gases are introduced systematically into the detection chamber in order to measure the scattering cross section more precisely.

The REMPI spectrum shown in Fig. 1(b) indicates that the lowest rotational states of *ortho* ($|N = 0, K = 0\rangle$) and *para* ($|N = 1, K = 1\rangle$) CH_3 enter the trap region, and are trapped simultaneously. The trap decay shown in Fig. 3(b) is an average signal of these two species, because we used the Q branch for the detection in order to obtain stronger trap signals. The trap lifetime of these two species must be different due to the difference in the interaction; the interaction in the *para* species is more anisotropic than that in the *ortho* species. Further improvement in our sensitivity to detect each spin component separately is underway in order to reveal the role of anisotropy of the interaction potential in molecular collisions, which is intrinsic to different rotational states of molecules.

Since the cross section of the multi-photon ionization we used in this study is not known, it is difficult to estimate the density of the radicals in the trap at this moment. The evaluation of the density via cavity enhanced IR absorption spectroscopy is the next experiment we are planning. Further cooling via evaporative (and/or, to a lesser extent, sympathetic cooling) requires a certain density such that enough number of collisions take place during the cooling process [32].

Our simulation shows that the velocity deviation of CH_3 in the present trap is about $\pm 10 \text{ m s}^{-1}$, corresponding to a translational temperature of 200 mK (FWHM) in the trap. The thermal de Broglie wavelength of CH_3 at this temperature is 1.0 nm, which is already a few times larger than the classical molecular size of CH_3 (0.4 nm). It is expected that a deviation in the collisional behavior from high-temperature (high velocity) collisions will be observed. Control and acceleration of cold reactions of molecules in an optical trap by external magnetic fields via Feshbach resonances, such as the formation of C_2H_6 from two CH_3 radicals, is one of the important topics of ultracold chemistry to be explored.

In conclusion, an ensemble of cold CH_3 radicals at 200 mK was created and successfully trapped in a magnetic trap for one second. In particular, being a different type of molecule from those for which trapping has been demonstrated, the trapping of CH_3 radicals provides many opportunities in the study of cold molecules, especially for making ultracold ensembles of polyatomic molecules towards BEC and for the investigation of cold collisions in the sub-kelvin regime.

The study was supported by a National Science and Engineering Research Discovery Grant in Canada and funds from Canada Foundation for Innovation for the Centre for Research on Ultra-Cold Systems (CRUCS) at UBC. The visit of David Carty was supported by the EPSRC Programme Grant MMQA: MicroKelvin Molecules in a Quantum Array (EP/I012044/1).

[1] M. H. Anderson, J. R. Ensher, M. R. Matthews, C. E. Wieman, and E. A. Cornell, *Science* **269**, 198 (1995).
 [2] K. Davis, M. Mewes, M. Andrews, N. van Druten, D. Durfee, D. Kurn, and W. Ketterle, *Phys. Rev. Lett.* **75**, 3969 (1995).
 [3] R. V. Krems, W. C. Stwalley, and B. Friedrich, eds., *Cold Molecules: Theory, Experiment, Applications* (CRC Press, Boca Raton, USA, 2009).
 [4] L. D. Carr, D. DeMille, R. V. Krems, and J. Ye, *New J. Phys.* **11**, 055049 (2009).
 [5] D. S. Jin and J. Ye, *Chem. Rev.* **112**, 4801 (2012).
 [6] J. J. Hudson, D. M. Kara, I. J. Smallman, B. E. Sauer, M. R. Tarbutt, and E. A. Hinds, *Nature Phys.* **473**, 493 (2011).

[7] The ACME Collaboration, J. Baron, W. C. Campbell, D. DeMille, J. M. Doyle, G. Gabrielse, Y. V. Gurevich, P. W. Hess, N. R. Hutzler, E. Kirilov, I. Kozyryev, B. R. O’Leary, C. D. Panda, M. F. Parsons, E. S. Petrik, B. Spaun, A. C. Vutha, and A. D. West, *Science* **343**, 269 (2014).
 [8] I. W. M. Smith, ed., *Low Temperatures And Cold Molecules* (World Scientific, 2008).
 [9] S. Ospelkaus, K. K. Ni, D. Wang, M. H. G. de Miranda, B. Neyenhuis, G. Quémener, P. S. Julienne, J. L. Bohn, D. S. Jin, and J. Ye, *Science* **327**, 853 (2010).
 [10] E. Lavert-Ofir, Y. Shagam, A. B. Henson, S. Gersten, J. Kłos, P. S. Żuchowski, J. Narevicius, and E. Narevicius, *Nature Chemistry* **6**, 332 (2014).
 [11] N. Balakrishnan and A. Dalgarno, *Chem. Phys. Lett.* **341**, 652 (2001).
 [12] G. Quémener and P. S. Julienne, *Chem. Rev.* **112**, 4949 (2012).
 [13] S. Y. T. van de Meerakker, H. L. Bethlem, N. Vanhaecke, and G. Meijer, *Chem. Rev.* **112**, 4828 (2012).
 [14] N. Vanhaecke, U. Meier, M. Andrist, B. H. Meier, and F. Merkt, *Phys. Rev. A* **75**, 031402 (2007).
 [15] E. Narevicius, A. Libson, C. G. Parthey, I. Chavez, J. Narevicius, U. Even, and M. G. Raizen, *Phys. Rev. Lett.* **100**, 093003 (2008).
 [16] E. Narevicius, A. Libson, C. Parthey, I. Chavez, J. Narevicius, U. Even, and M. Raizen, *Phys. Rev. A* **77**, 051401 (2008).
 [17] A. W. Wiederkehr, H. Schmutz, M. Motsch, and F. Merkt, *Mol. Phys.* **110**, 1807 (2012).
 [18] Y. Liu, S. Zhou, W. Zhong, P. Djuricanin, and T. Momose, *Phys. Rev. A* **91**, 021403(R) (2015).
 [19] T. Momose, Y. Liu, S. Zhou, P. Djuricanin, and D. Carty, *Phys. Chem. Chem. Phys.* **15**, 1772 (2013).
 [20] M. J. McEwan and L. F. Phillips, *Chemistry of the Atmosphere* (Edward Arnold Publishers, London, 1975).
 [21] A. W. Jasper, S. J. Klippenstein, L. B. Harding, and B. Ruscic, *J. Phys. Chem. A* **111**, 3932 (2007).
 [22] C. Yamada, E. Hirota, and K. Kawaguchi, *J. Chem. Phys.* **75**, 5256 (1981).
 [23] M. Jacox, *J. Phys. Chem. Ref. Data* **32**, 1 (2003).
 [24] S. Hoekstra, J. J. Gilijamse, B. Sartakov, N. Vanhaecke, L. Scharfenberg, S. Y. T. van de Meerakker, and G. Meijer, *Phys. Rev. Lett.* **98**, 133001 (2007).
 [25] T. V. Tscherbul, H. G. Yu, and A. Dalgarno, *Phys. Rev. Lett.* **106**, 073201 (2011).
 [26] Y. Miyamoto, M. Fushitani, D. Ando, and T. Momose, *J. Chem. Phys.* **128**, 114502 (2008).
 [27] J. T. Hougen and T. Oka, *Science* **310**, 1913 (2005).
 [28] Z.-D. Sun, K. Takagi, and F. Matsushima, *Science* **310**, 1938 (2005).
 [29] T. Kravchuk, M. Reznikov, P. Tichonov, N. Avidor, Y. Meir, A. Bekkerman, and G. Alexandrowicz, *Science* **331**, 319 (2011).
 [30] J. F. Black and I. Powis, *J. Chem. Phys.* **89**, 3986 (1988).
 [31] J. Van Dongen, C. Zhu, D. Clement, G. Dufour, J. L. Booth, and K. W. Madison, *Phys. Rev. A* **84**, 022708 (2011).
 [32] B. K. Stuhl, M. T. Hummon, M. Yeo, G. Quemener, J. L. Bohn, and J. Ye, *Nature* **492**, 396 (2012).